Ahead of print

Med Ultrason 2023:0, 1-13 Online first
DOI: 10.11152/mu-4260

Comments and illustrations of the WFUMB CEUS liver guidelines: Rare benign focal liver lesion, part I

Yi Dong[1], Wen-Ping Wang[2], Ehsan Safai Zadeh[3], Kathleen Möller[4], Christian Görg[3], Annalisa Berzigotti[5], Nittin Chaubal[6], Xin Wu Cui[7], Chiara De Molo[8], Klaus Dirks[9], Nathally Espinosa Montagut[10], Odd Helge Gilja[11], Alois Hollerweger[12], Christian Jenssen[13], Ernst-Michael Jung[14], Christoph Klinger[15], Adrian Lim[16], Vito Sansone[17], Andreas Schuler[18], Carla Serra[8], Zeno Sparchez[19], Christoph Frank Dietrich[20]

[1]Department of Ultrasound, Xinhua Hospital Affiliated to Shanghai Jiaotong University School of Medicine, Shanghai, China, [2]Department of Ultrasound, Zhongshan Hospital, Fudan University, Shanghai, China, [3]Department of Biomedical Imaging and Image-Guided Therapy, Medical University of Vienna, Vienna, Austria, [4]Medical Department I/ Gastroenterology; SANA Hospital Lichtenberg, Berlin, Germany, [5]Department of Visceral Surgery and Medicine, Inselspital, Bern University Hospital, University of Bern, Bern, Switzerland, [6]Thane Ultrasound Centre, Jaslok Hospital and Research Centre, Mumbai, India, [7]Department of Medical Ultrasound, Tongji Hospital, Tongji Medical College, Huazhong University of Science and Technology, Wuhan, China, [8]Interventional, Diagnostic and Therapeutic Ultrasound Unit, Department of Medical and Surgical Sciences, IRCCS, Azienda Ospedaliero-Universitaria Sant'Orsola Malpighi Hospital, Bologna, Italy, [9]Rems-Murr-Klinikum, Winnenden, Germany, [10]School of Medicine, Universidad de los Andes, Bogotá, Colombia, [11]National Centre for Ultrasound in Gastroenterology, Haukeland University Hospital, Bergen, and Department of Clinical Medicine, University of Bergen, Norway, [12]Department of Radiology and Nuclear Medicine, Barmherzige Brüder Hospital Salzburg, Austria, [13]Medical Department, Krankenhaus Maerkisch-Oderland, Strausberg, Germany, and Brandenburg Institute of Clinical Ultrasound at Medical University Brandenburg, Neuruppin, Germany, [14]Department of Radiology, University Medical Center Regensburg, Germany, [15]Vaisana Ärztehaus GmbH, Vaihingen/Enz, Germany, [16]Imperial College London and Healthcare NHS Trust, London, UK, [17]Unit of Internal Medicine, Department of Medical and Surgical Sciences, University of Bologna S. Orsola-Malpighi Hospital, Bologna, Italy, [18]Zentrum für Innere Medizin, Alb Fils Kliniken, Helfenstein Klinik, Germany, [19]Department of Internal Medicine-Gastroenterology, University of Medicine and Pharmacy, Cluj-Napoca, Romania, [20]Department Allgemeine Innere Medizin, Kliniken Hirslanden, Beau Site, Salem und Permanence, Bern, Switzerland

Abstract

Improved detection and characterization of common focal liver lesions (FLL) are the main topics of the World Federation for Ultrasound in Medicine and Biology (WFUMB) guidelines on the use of contrast-enhanced ultrasound (CEUS). On state-of-the-art CEUS imaging, to create a library of rare FLL, especially concerning their atypical imaging characteristics, might be helpful for improving clinical diagnostic efficiency. In this review, we aim to summarize the ultrasound and CEUS features of rare benign FLL. Currently there are limited reports and images published.

Keywords: Focal liver lesions (FLL); ultrasound; contrast enhanced ultrasound (CEUS); detection; guidelines

Received 20.03.2023 Accepted 22.05.2023
Med Ultrason
2023:0 Online first, 1-13
Corresponding author: Christoph F Dietrich
Department Allgemeine Innere Medizin (DAIM),
Kliniken Hirslanden Beau Site,
Salem und Permancence, Bern, Switzerland
Phone: +41764408150
E-mail: ChristophFrank.Dietrich@hirslanden.ch
ORCID: http://orcid.org/0000-0001-6015-6347

Introduction

According to the published guidelines on the use of contrast-enhanced ultrasound (CEUS) for the evaluation of focal liver lesions (FLL) by World Federation for Ultrasound in Medicine and Biology (WFUMB) [1-5] improved detection and characterization of common FLL are the main topics. In recent years, some published

literatures described imaging features of conventional ultrasound (US) and CEUS of less common FLL [6-12].

FLL with different histopathological diagnosis might show various common and uncommon imaging features. Some similar imaging features could be observed in different histopathology. Clinically, it is necessary to accurately characterize FLL as benign or malignant lesions, which may have impact on different clinical management. On state-of-the-art CEUS imaging, most FLL can be detected and characterized with confidence according to current well-known WFUMB guidelines [4,5]. However, atypical imaging characteristics in some rare lesions may bring clinical diagnostic difficulties [6-20]. Published papers with gold-standard histology cover cholangiocellular adenoma [21], peliosis [22-24], cystadenoma and cystadenocarcinoma [25], hemangioendothelioma [26,27], and hepatocellular carcinoma (HCC) in the non-cirrhotic liver [8,14,28,29] and how to deal with incidental findings in general [30]. There are also several papers reporting on the rare and more esoteric hepatic lesions. These papers include characterization of fibrolamellar hepatocellular carcinoma [16,31], very small HCC (<10 mm) [32], mixed HCC and cholangiocellular carcinoma [33], nodular regenerative hyperplasia [34], sarcoma [35], inflammatory pseudotumour [36], sarcoidosis [37-40], tuberculosis [41,42], hydatid cysts [43-46], alveolar echinococcosis [44], schistosomiasis [47,48], ascariasis [49,50], fasciolosis [51], clonorchis and opisthorchis [52], toxocariasis [53], bacillary angiomatosis [54], amyloidosis with spontaneous hemorrhage [55], and portal venous gas accumulation [20] and rare FLLs in pediatric patients [56,57].

In this series of reviews, we aim to summarize both the US and the CEUS features of those rare and very rare FLL in order to create a library of these rare lesions. Up till now, there are limited reports published.

Hepatocellular adenoma, new classification

Hepatocellular adenoma (HCA) is a rare benign FLL primarily detected in women. It is proved to be associated with the use of anabolic steroids and estrogen-containing oral contraceptives, and it is more frequent in patients with glycogen storage liver diseases and Abernethy malformation [58,59]. Additional causal factors include obesity and alcohol [58,59]. HCAs can be single or multiple, and the term "adenomatosis" is used to define the presence of more than 10 HCAs in the liver. The latter situation is most commonly observed in glycogen storage liver diseases. Whereas larger lesions may cause right upper abdominal discomfort or pain, HCAs with a diameter <5 cm are usually asymptomatic and detected incidentally; In 20-27% of cases bleeding may occur, and rupture and bleeding into the abdominal cavity have been described in exophytic cases [60]. The risk of bleeding is associated with larger size (>5 cm), growth rate, exophytic lesions, visible vascularity, chronic alcohol consumption and two types of mutation: sonic hedgehog mutation and exon 7/8 mutation of the β-catenin-pathway. In about 5-8% of the patients, malignant transformation of the HCA into HCC may occur, most frequently in males with lesions >5 cm in diameter [61]; the risk is strictly associated with 2 mutations of the β-catenin-pathway: TERT promoter mutations and CTNNB1 exon 3 mutations [58,59,62].

Classification

HCAs can be classified into five main subgroups [58,59,62-64], each with distinctive molecular or histological features and may exhibit different clinical manifestations [58,65,66]: 1) inflammatory (30-40 % of all HCAs), histologically displaying marked inflammatory infiltrates and overexpression of acute-phase inflammatory proteins [67]; 2) hepatocyte nuclear factor 1 alpha (HNF1A)-inactivated (35-45% of cases), characterized by the bi-allelic inactivation mutation of HFNF1A and a high fat component [68]; 3) β-catenin-mutated (≈10% of cases), associated with a higher risk of malignant transformation [69]; 4) sonic hedgehog activated (≈ 4% of cases) and 4) unclassified (5-10% of cases), associated with less common genetic mutations [58,59].

Imaging

Features of HCA in US imaging are non-specific, and this tumor may present as a hyper- or hypoechoic or an inhomogeneous focal lesion. The hyperechoic aspect is frequently observed in HFNF1A HCAs, due to their fat content [60]. The typical CEUS enhancement pattern of HCA includes rapid centripetal filling in the arterial phase and persistent hyperenhancement in the portal venous and late phases [64,70]. The centripetal filling derives from the subcapsular feeding arteries [2]. Diffuse enhancement may occur somewhat less frequently, while centrifugal flooding has rarely been described [64,70]. However, mixed filling in the arterial phase is not uncommonly observed [71,72]. The filling is usually complete, but non-enhancing areas due to previous bleeding have also been observed. HCA showed no specific filling patterns in the arterial phase, which is also similar in HCC or in hypervascularized metastasis [2].

Depending on the subtype, all inflammatory HCAs are hyperenhanced in the arterial phase, while more than half of the HNF1A-inactivated HCA and ß-catenin-mutated HCA cases are isoenhanced. None of the adenomas display hypoenhancement in the arterial phase [73]. In the portal venous and late phases, HCAs are typically mildly hypoenhancing (i.e., slow and mild washout),

resulting in a difficult differential diagnosis from HCCs [71,74,75]. In other studies, and reports, HCAs examined with SonoVue exhibit general washout in the portal venous and late phases, which can be explained by the lack of portal vein branches. Those examined with Levovist or Sonazoid may present with iso- or hyperenhancement.

It has been proposed that the heterogeneous dynamic enhancement pattern of HCA in CEUS, particularly in the portal venous and late phases, could depend upon the molecular features of the tumor, which differ among the various subtypes [76]. According to Laumonier et al's study, in the portal venous phase, 15 out of 16 HNF1A-inactivated HCAs were isoechoic and 1 was hypoechoic compared to the surrounding liver parenchyma. In the late venous phase, 14 of the 16 reported HNF1A-inactivated HCAs were isoenhancing in comparison to the non-tumoral liver. The remaining two HNF1a-inactivated HCAs were hypoenhancing [73]. In the same study, among the 17 reported inflammatory HCAs, the majority (65%; 11 out of 17) were hypoenhancing in the late venous phase, and only 23% (4/17) were isoenhancing; 29% (5/17) of the inflammatory HCAs displayed persistent hyperenhancement in the portal phase, compared to only 12% (2/17) in the late phase. In 13 of hypo- or isoenhancing inflammatory HCAs, a rim of persistent enhancement was observed [73].

In an Italian multicenter study using CEUS, during the arterial phase, all but one HCAs (94.7%] displayed rapid arterial enhancement; 89% of them exhibited a centripetal and 11% a centrifugal filling pattern. The only lesion without arterial enhancement was an unclassified HCA. During the portal and/or late venous phase, 58% of HCAs presented with complete or partial and mainly central washout, and the remaining 42% displayed persistent enhancement. In particular, among inflammatory HCAs, 7 out of 14 exhibited no washout, while 3 displayed wash-out in the portal venous/late phases and 4 displayed wash-out in the late phase only, respectively. The ß-catenin-mutated HCA and all but 1 unclassified HCAs presented with portal or late washout [64] (fig 1-4).

The series from Manichon et al indicates that late washout was observed only in a minority of inflammatory and HNF1A-inactivated HCAs [77]. The CEUS enhancement patterns of β-catenin-mutated and unclassified HCAs has been reported in relatively few cases showing arterial hyperenhancement in all cases and various enhancement patterns in portal and late phase [73,77]. Magnetic resonance imaging (MRI) enhanced by liver-specific contrast agents such as gadoxetic acid (Primovist®) may be considered. The advantage of MRI in subtyping is to combine the detection of typical mor-

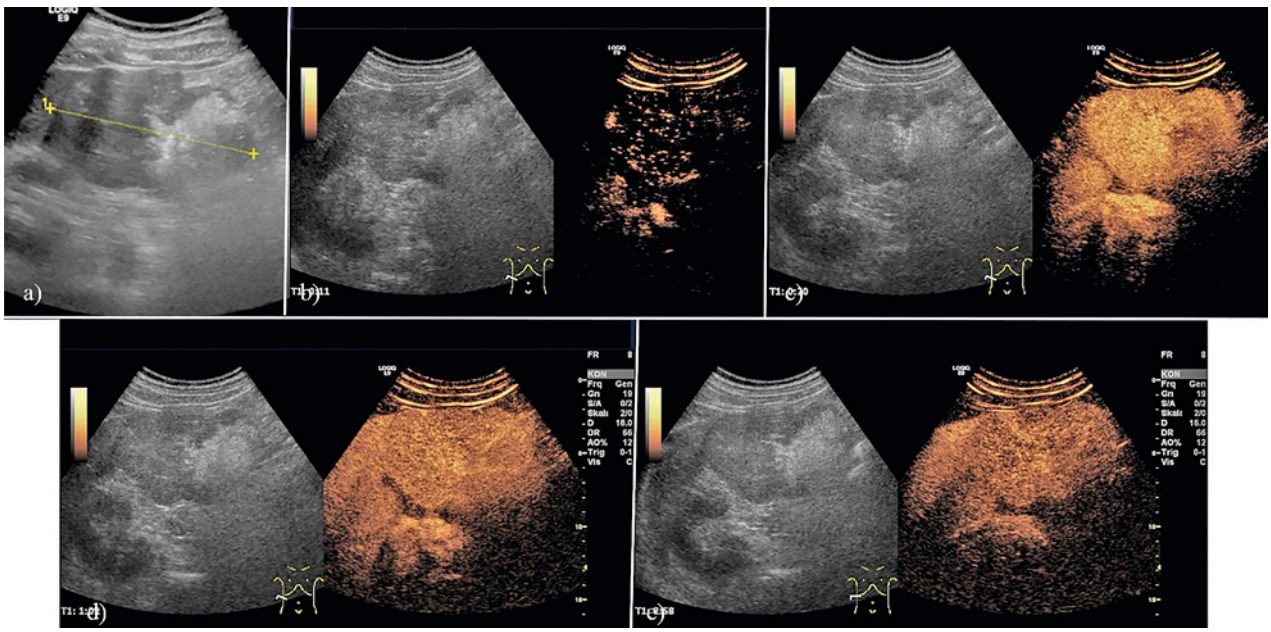

Fig 1. ß-catenin-mutated hepatocellular adenoma, 55 y/o male presenting with non-specific abdominal complaints. Alcohol abuse was known but no cirrhosis of the liver. B-mode ultrasound revealed an 11 cm smooth bordered inhomogeneous mass in the right lobe of the liver, with hypoechoic, but also with hyperechoic parts and calcification (a). On CEUS, the lesion showed diffuse reticular contrast enhancement in the early arterial phase (b). In the arterial phase, the lesion was completely and homogeneously hyperenhanced (c). In the portal venous phase, the lesion was only minimally hypoenhanced (d) and showed slight hypoenhancement in the late phase (e).

phological features as fat and vascular spaces with phase-specific enhancement patterns and fractal analysis [78]. However, in one current meta-analysis on the role of hepatobiliary phase iso- or hyperintensity on gadoxetic acid-enhanced MRI in diagnosis of HCA including data from 410 HCAs from 28 studies and case reports, only 8% were ß-catenin-mutated HCA and 15% unclassified HCA. Compared to none of HNF1A-inactivated HCAs, 59% of ß-catenin-mutated HCAs were iso- or hyperintense in hepatobiliary phase of gadoxetic acid-enhanced

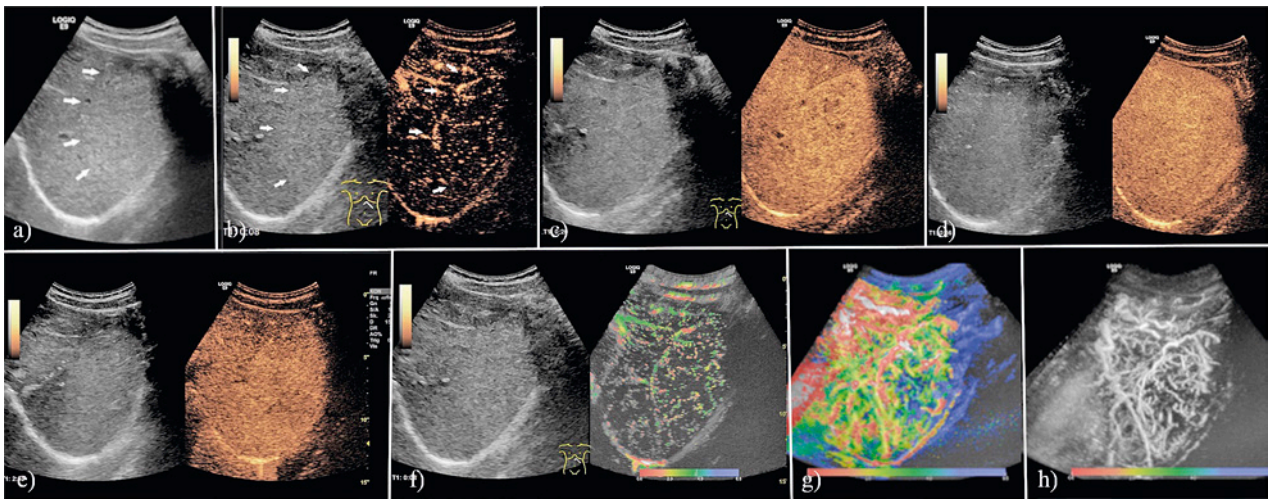

Fig 2. Inflammatory hepatocellular adenoma histologically confirmed and surgically resected, 35 y/o female. Feeling of pressure in the upper abdomen, palpable lesion in the epigastrium. B-mode ultrasonography showed a 9 cm smooth-bordered, slightly hyperechoic FLL in the left liver lobe (a). CEUS showed a reticular enhancement pattern in the early arterial phase (b). The lesions proved to be hyperenhancing in the arterial phase, (b) isoenhancing in the portal phase (d), and hyperenhanced in the late phase (e). Parametric imaging reveals the diffuse multifocal inflow pattern in the early arterial phase (f). Accumulation indicates some vessels in the rim of the FLL (g and h).

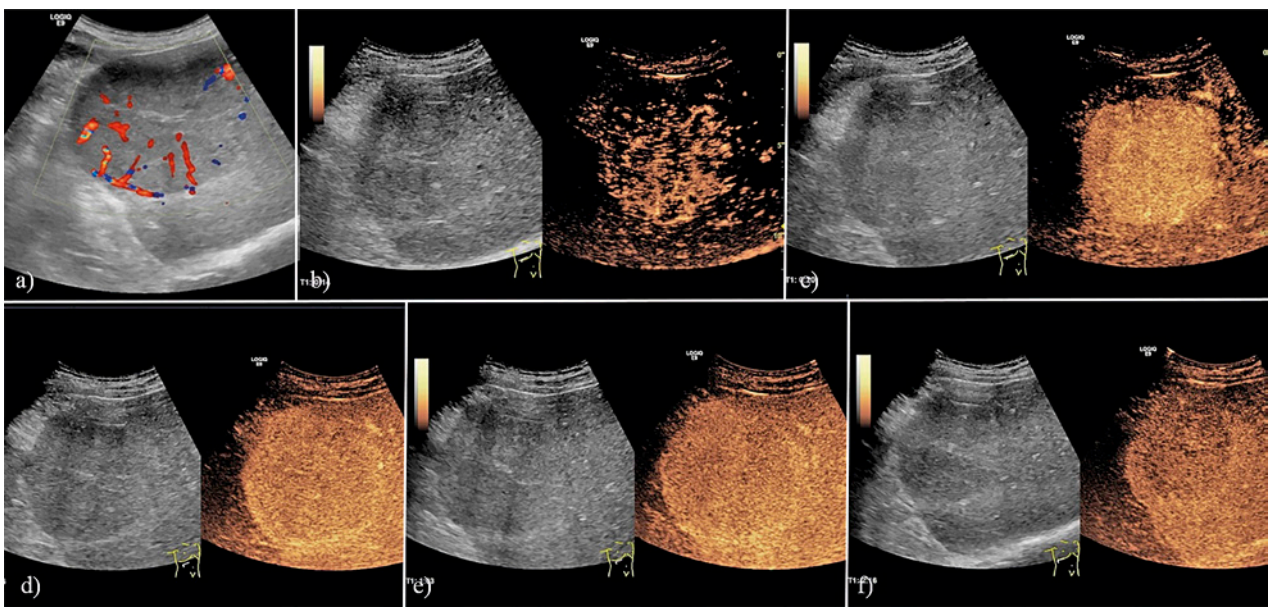

Fig 3. Inflammatory hepatocellular adenoma, surgically resected (under suspicion of hepatocellular carcinoma in a non-cirrhotic liver), 56 y/o male. Incidental finding of a slightly hypoechoic 8 cm FLL in the right lobe of the liver, with smooth borders. Color Doppler imaging demonstrated vessels radiating in from the periphery (a). In CEUS, the lesion demonstrates early and mild hyperenhancement in the arterial phase starting from the edge (b) but then becoming diffuse and homogeneous hyperenhanced (c). In the portal venous phase, the lesion is isoenhanced with hyperenhanced rim (d) and somewhat later in the portal venus phase mild hypoenhanced with persisting rim hyperenhancement. (e). In the late phase, the lesion is hypoenhanced (f).

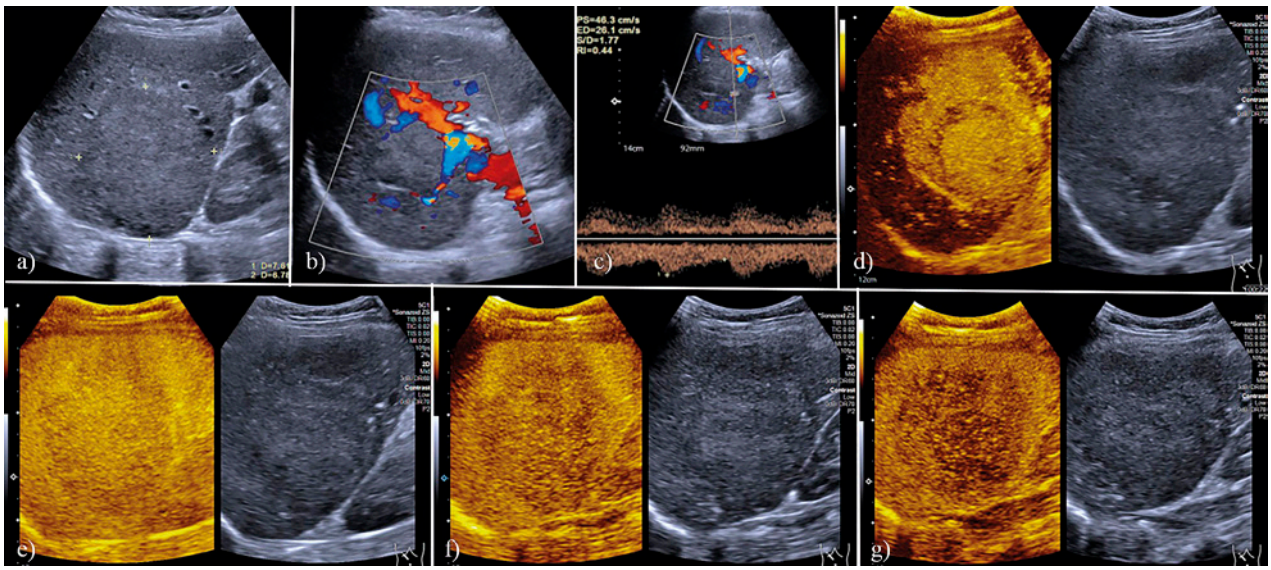

Fig 4. A 30-year-old female with incidental focal liver lesion. A heterogeneously hypoechoic solid lesion with a regular shape and well-defined margin was detected in the right lobe of liver (a). Color flow signal was detected within the lesion (b) with a low resistance index (RI = 0.44) (c). After injection of contrast agent (Sonazoid), the lesion showed heterogeneous hyperenhancement during the arterial phase (d), hypoenhancement during the portal venous phase (e), late phase (f) and Kupffer phase (g). The molecular unclassified lesion was surgically resected and histopathology revealed the diagnosis of hepatic adenoma.

MRI. Specificity of hepatobiliary phase iso- or hyperintensity on gadoxetic acid-enhanced MRI for differentiating FNH from ß-catenin-mutated and unclassified HCA subtypes was only 65% [79]. Irrespective of the subtype, iso- or hyperintensity on gadoxetic acid-enhanced MR in otherwise diagnosed HCA can be regarded as a highly specific marker for ß-catenin activation (97% specificity) and, therefore, predictive of high malignancy risk [80].

In the literature there are different arterial and portal venous phase enhancement patterns described. The discrepancies can be explained by different types of HCAs in different underlying diseases including congenital etiology, different stages of steatosis, fibrosis and cirrhosis of the surrounding liver parenchyma. In addition, pathologists may differ in the gold standard criteria of HCA and FNH. Biopsy and histological and molecular classification using an immunohistochemistry panel of 5 markers should be done in all suspected HCA <5 cm and surgical resection should be done in all suspected hepatocellular adenoma >5 cm or in growing lesions. Surgical resection should be done irrespective of the size in male patients and in case of proven β-catenin-mutated HCAs [78].

Von Meyenburg malformation (Bile duct hamartoma)

Bile duct hamartomas (BDHs), also known as von Meyenburg malformations or von Meyenburg complexes (VMCs), are considered a benign form of embryonic ductal plate malformation. Embryonic ductal plate malformations include Caroli disease and syndrome, various polycystic liver and kidney diseases, as well as biliary atresia and congenital liver fibrosis. BDHs may be isolated or associated with one or more of these embryonic ductal plate malformations. They were first reported by Eli Moschcowitz in 1906 and established by the Swiss pathologist Hanns von Meyenburg in 1918 [81,82]. Von Meyenburg complexes are usually rare incidental findings.

In an autopsy series (n = 2843), BDHs were diagnosed in 5.6% of adults and in 0.9% of children [83, 84]. VMCs are mostly multiple tiny lesions that present under the liver capsule or inside the liver. The lesions are usually very small, with sizes of up to 15 mm. Smaller lesions up to 5 mm may not be visible through imaging. Multiple hamartomas occur in both lobes of the liver. Single hamartomas have been reported; they may be larger and present in the peripheral region of the liver in most cases [85].

VMCs are lesions consisting of malformed bile ducts of varying calibers in a densely collagenized stroma. The ductal structures are often variably wide, narrow, or dilated and contain bile, protein, or colloid components. Pronounced dilatation may assume a cystic appearance. The connective tissue stroma around the ducts is denser compared to the normal portal tracts and often appears hyalinized. The stroma of the lesions can become extensively hyalinized, and the ductal structures are atrophic and can hardly be delimited. The ducts may disappear completely, leaving a sclerotic hyaline nodule. In this

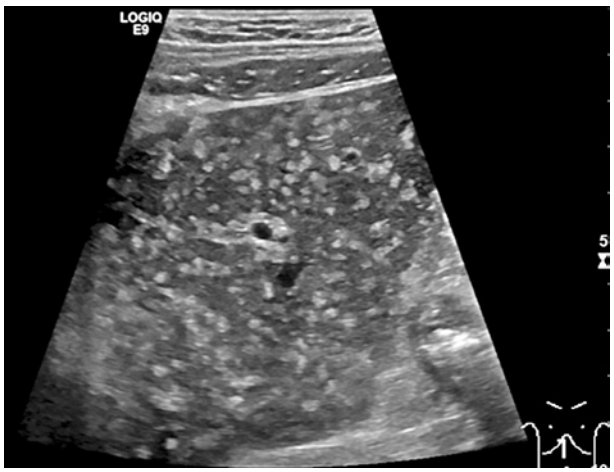

Fig 5. Von Meyenburg complexes histological proven in a 66-year-old male patient. Incidental finding in a patient with acute pancreatitis. The entire liver parenchyma is interspersed with multiple small hyperechoic foci.

case, the VMCs appear solid rather than cystic. Therefore, both cystic and solid lesions are present during imaging. VMCs have no connection to the biliary system [84]. There are some pathological reports with indirect evidence for neoplastic progression of VMCs to (in particular small duct type) intrahepatic cholangiocarcinoma with especially ARIDA1 mutations being involved in this process [86-88]. Therefore, VMCs are considered as potential precursor lesion of intrahepatic cholangiocellular carcinoma (ICC) and surveillance should be considered on an individual basis [89].

Imaging

Typical appearances in US images include a heterogeneous pattern of the liver, multiple tiny hyperechoic or hypoechoic lesions, small cysts, and multiple comet-tail-like artifacts. The low-echo lesions may have a narrow hypoechoic rim. Variations in imaging features may be explained by the differences in size and number of the dilated bile ducts (hypoechoic lesions on US) as well as the variable density of the fibrous tissue surrounding them (hyperechoic lesions on US). So, on US scan, VMC may be confused with liver metastases, micro-abscesses, biliary stones, or fibrosis [84,90-94].

Solitary BDHs may display various types of echogenicity depending on the levels of bile duct outgrowth, fibrous stroma, cystic bile duct dilatation, and the bile and protein contents of the mass. They can be both hy-

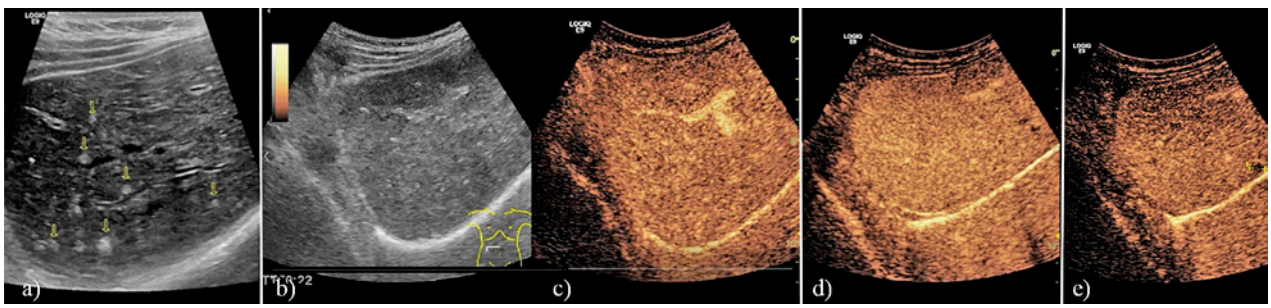

Fig 6. Von Meyenburg malformation (histological proven), 48 y/o female. Non-specific abdominal complaints. B mode ultrasound shows multiple hyperechoic lesions (arrows) <5 mm and tiny cysts <5 mm (a). CEUS showed isoenhancement in the arterial (b), portal venous (c) and late phase. The cysts around 5 mm were non-enhanced (d).

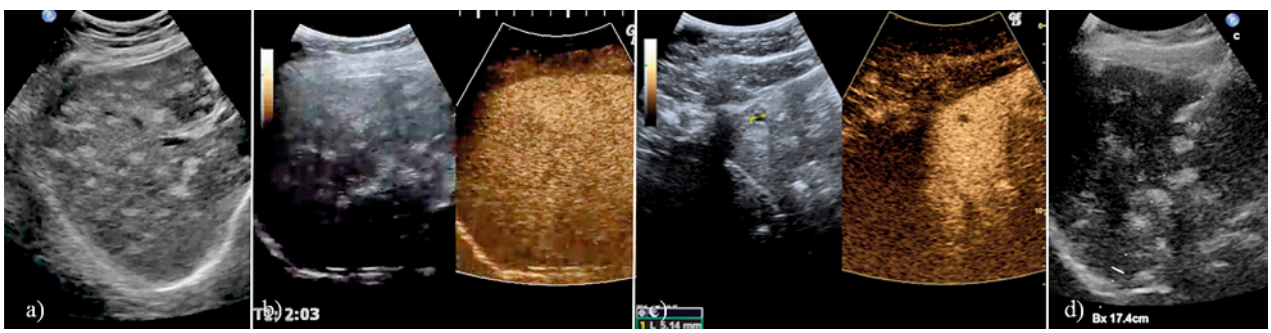

Fig 7. Von Meyenburg complexes (histological proven), 60-year-old, female, presenting with epigastric pain. The patients is on Tamoxifen treatment due to breast cancer diagnosed 2 years earlier. Normal liver enzymes. Ultrasound demonstrates innumerable, tiny, hyperechoic lesions throughout the entire liver (a). At CEUS all lesions are isoenhancing throughout all vascular phases (b), except for one subcentimetric simple cyst without any enhancement (c). Due to the history of breast cancer percutaneous US-guided biopsy (d) was performed twice, both without proof of malignancy. On ultrasound follow-up after one year and clinical follow-up after 12 years, the patient is without malignant disease.

poechoic and hyperechoic in appearance [85]. No vessels are visible in the lesions on Color and Power Doppler ultrasound [91,95]. The few reports using CEUS describe different characteristics depending on the contrast agent used. In a report using SonoVue in a single 5-mm biliary hamartoma, the lesion in the arterial and portal venous phases exhibited slightly less enhancement than the surrounding tissue. In the late phase (>2 min), the lesion disappeared completely, presenting a similar degree of enhancement as the surrounding liver parenchyma. Washout in the late phase was observed in the same lesion with Levovist [91]. It must be noted that the smallest lesions below 5 mm may escape the resolution of CEUS [91]. In other reports using CEUS with sulfur hexafluoride, no appreciable vascularity was observed within the hepatic lesions in all three phases of the study for an imaging duration of 3 min [95]. This may represent the non-enhancing character of the lesions, and it may be explained by the microscopic cyst-like structure of the malformations. A weak septum-like structure in a single lesion was also found in CEUS with Sonazoid [85].

The clinical significance of VMCs is their differentiation from other clinically significant focal liver lesions. These include, for example, liver metastases, other liver malignancies, and micro-abscesses. For patients with VMCs, an increase in the tumor marker CA19-9 was described without the presence of a malignant tumor [94] (fig 5-7).

Mucinous cystic neoplasm of the liver

Mucinous cystic neoplasm of the liver (MCN-L) are rare cystic hepatic neoplasms which are usually multilocular. Previously they were also known as intrahepatic biliary cystadenomas or cystadenomas. Clinical, radiological, and histological features of those lesions are nonspecific to reach an accurate diagnosis [25,96]. According to an analysis of a large group of resected liver cysts ≥1 cm, only 13 % of all liver cysts are neoplastic. The largest group (10.5%) are MCN-L. They are characterised by their ovarian stroma, occur (almost) exclusively in women and unifocally, and have a lower malignancy rate (7%) than their pancreatic counterparts. The majority of liver cysts are non-neoplastic (87%), including infectious/inflammatory (12%, e.g. echinococcal), congenital (7%) and other benign cysts (4%). The largest group (63%) are cystic bile duct hamartomas and benign bile duct liver cysts not otherwise specified, which are associated with ductal plate malformation, are large, female predominant and typically multifocal, and are often misdiagnosed as "hepatobiliary cystadenoma" on imaging [96]. In contrast to MCN-L, intraductal papillary neoplasms (IPNB) develop in the extra- or larger intrahepatic bile ducts and very rarely have the appearance of a liver cyst.

Imaging

Thin-walled MCN-L are usually filled with watery fluid. In some cases, the cyst wall may be thickened, may show papillary structures and filled with thicker mucinous fluid. They range in size from several mm up to 28 cm. As histopathologic results show, the cystic spaces are lined by cuboidal to columnar often monolayer mucin-secreting epithelium and ovarian-type stroma is seen subepithelial [97-99].

However, in male patients ovarian-type stroma may not be obvious in some cases. In MCN-L, the typical densely cellular ovarian-type stroma is a specific feature that the lesion share with their counterparts in the pancreas. This distinctive stroma is exclusively present in female patients. It is immunoreactive, potentially positive for synaptophysin and vimentin, positive for estrogen as well as for alpha-inhibin, negative for progesterone receptors [100]. These tumors are much more common in young to middle aged women. Although some patient may present with more specific symptoms, such as jaundice, most of patients often show nonspecific syndromes, such as abdominal discomfort. Clinically, these tumors are often misdiagnosed as simple liver cysts on imaging studies such as US, endoscopic retrograde cholangiopancreatography (ERCP), and computed tomography (CT) scan. Comparing to other imaging methods, CT is more accurate in demonstrating size and anatomic extent of these lesions, while US is more sensitive in detecting septa in cystic lesions. On CT typical MCN-L ("biliary cystadenomas") are isodense to water (less than 30 HU) with nodular areas enhancing with intravenous contrast. Biliary duct dilatation, single cysts, and lesions in the left lobe of the liver can be predictive for the diagnosis. [99,101].

The potential of CEUS is to reveal vascularization of septa with high sensitivity as well as in even small nodules within the cystic lesion. Differential diagnosis like simple liver cysts, Echinococcosis or non-vascularized septa or nodules of mucin in cysts of other origin can be excluded when vascularization of septa or nodules is documented with CEUS. Xu et al described that contrast-enhancing nodules >10 mm already tend to indicate carcinoma as well as the ratio of cystic to solid parts of <1. Nodes <10 mm and predominantly cystic portions were more typical of a cystadenoma [102]. For malignant lesions, both ERCP and MRCP can assess the biliary and pancreatic ducts for possible tumor invasion, with MRCP may provide additional information about the biliary tree proximal to any obstruction [103]. In fact, multiple in-

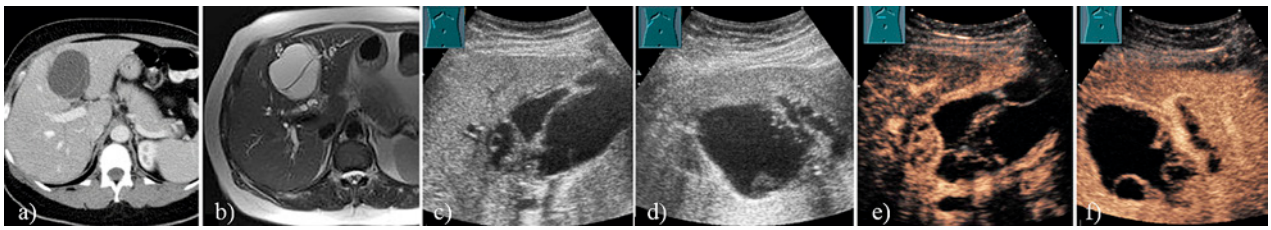

Fig 8. Mucinous cystic neoplasia of the liver (MCN-L). A 57-year-old female patient with a complex cystic lesion and upper abdominal pain. Visualization of the lesion on computed tomography (courtesy of Prof. Dr. Mahnken, Department of Radiology, University Hospital Marburg) (a), magnetic resonance imaging (b) and B-mode ultrasound (c,d). On CEUS the lesion showed marked enhancement after 30 s (e) and 1 min (f). Histologically, a diagnosis of MCN-L (hepatobiliary cystadenoma) was confirmed, followed by tumor resection.

vestigators have suggested that biliary cystic neoplasms (MCN-L) are more often located in the left hemi-liver. Therefore, complex cystic lesions of the left liver should be considered suspicious especially in the setting of an increase in alkaline phosphatase. While there have been anecdotal reports on its potential usefulness in identifying malignancy with biliary cystic adenocarcinomas, no definitive conclusions can be made regarding the utility of PET-CT for BCTs [101,104].

As extremely rare cystic lesions of the liver, intrahepatic biliary cystadenoma and cystadenocarcinoma are rarely reported. Also, it is a challenge to differentiate between the two lesions [104].

On radiological examination, tuberculosis of the liver may also mimic biliary cystadenomas. Due to their nonspecific clinical symptoms and imaging signs, they may be misdiagnosed as infectious diseases such as hydatid disease, treatment is often inadequate. Other potential differential diagnosis are metastases of malignant cystic ovarian masses (mostly mucinous adeno-carcinoma) or cystic endometriosis in the liver (very rare, progesterone receptor positive) [100]. Large papillary masses could often be detected in malignant cases. It is essential to make accurate diagnosis of these tumors. Preoperative CEUS (or CECT/CEMRI) imaging that demonstrates the presence of internal vascularized septa is highly suggestive of diagnosis of MCN-L. Owing to their potential of malignancy and high recurrence rate after incomplete resection, an aggressive approach is highly recommended.

In order to prevent recurrence or potential malignant transformation, it is commonly suggested that the lesion should be completely surgical removed by either liver resection or enucleation [105-108]. Nevertheless, other authors also recommending that marsupialization of the hepatic cysts may result in optimal outcome without tumor recurrence [109-111].

In recent decades, the emergence of laparoscopic techniques renders the surgeons more options regarding hepatic surgery. Since intrahepatic biliary cystadenomas are often detected in patients with non-cirrhotic liver

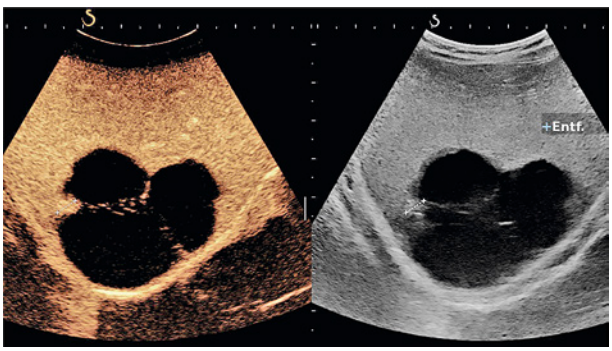

Fig 9. Cystadenoma (histological proven), 24-year-old, female with an incidental finding of a large cyst with nodules up to 12 mm. CEUS showed enhancement of noduli and septae as sign of neoplasia.

background, hepatic resection is considered to be relatively safe. Meanwhile, adequate future liver remnant is also reserved. For patients with history of hepatic viral infection and/or cirrhosis, liver functions measurements such as indocyanine green 15 min retention test (ICG-15), should be taken into consideration before radical hepatic resection. The outcome after radical hepatic surgery resection is usually good and satisfactory long-term outcome could be achieved [112]. New oral tyrosine kinase inhibitors such as Apatinib, which targets vascular endothelial growth factor receptor-2, is proved to be effective in treating the advanced intrahepatic biliary cystadenocarcinoma [113] (fig 8,9).

Pseudolipoma

Hepatic pseudolipoma, also referred to as pseudolipoma of the Glisson capsule (PGC), is an extremely rare benign tumor in primary hepatic lesions. The prevalence of hepatic pseudolipoma is 0.2% in a series of 1300 consecutive necropsies, and there have been 13 case reports to date. Its histological elements are identical to degenerating fat and fibrous capsules, and vascular supply via the liver capsule is possible. The reported size of PGC varies between 0.4 and 2 cm [114]. The size of migrating

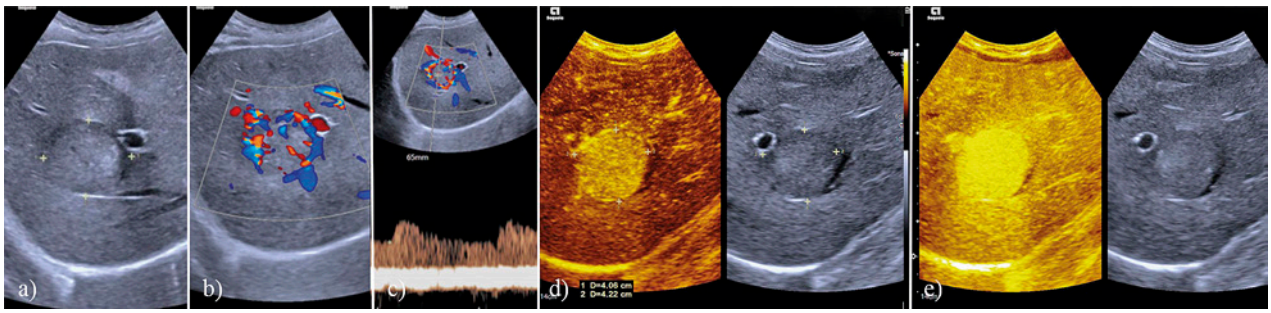

Fig 10. A 56-year-old man with incidentally diagnosed focal liver lesion. A hypoechoic lesion with regular shape and ill-defined margin was detected in the right lobe (a). Color flow signal was detected around the lesion (b) with low resistance index (RI=0.39) (c). After injection of contrast agent (Sonazoid), the lesion showed homogeneously hyperenhancement during early arterial phase (d), reached peak enhancement at 22 second (e), was hyperenhanced during portal venous phase (f) and hypoenhanced during late phase (g) and Kupffer phase. The lesion was resected, and histopathological results revealed a hepatic epithelioid angiomyolipoma.

loose bodies may be the critical factor for entry into the space between diaphragm and liver. Confusion with carcinoma metastasis, benign tumors, abscesses, and tuberculous nodule is common. PCG is usually firm, roundish, and partly embedded in the diaphragmatic surface of the liver, with a typically marginal groove, macroscopically resembling metastases. It manifests as a fibrous capsule surrounding mature, partly degenerating adipose tissue with fine fibrous septa, the color varies from white to grey or yellow. It is important to distinguish this condition from true lipoma, which has regular margins without a capsule and is located within the parenchyma. Pseudolipomas likely stem from epiploic appendages that have loosened, moved into the peritoneal cavity, and lodged between the liver and the diaphragm, receiving nutrition via the circulation of the liver [114]. Patients with PGCs have good prognoses [114], and no treatment is needed for this kind of tumor [114,115].

Imaging

On CT images, PGC lesions typically appear as well-circumscribed nodules with predominantly fat attenuation. Most PGC lesions are located on the diaphragmatic surface of the liver [115]. On PET-CT, the lesions are not FDG-avid, favoring a benign etiology [115]. To date, CEUS findings have not been reported in the literature.

Angiomyolipoma

Hepatic angiomyolipoma (hAML) is a rare benign mesenchymal liver tumor. Histopathologically, it is characterized by proliferating blood vessels with thick wall, smooth muscle and mature adipose cells (which can be from 5% to 90% of the tumor). Since it is usually asymptomatic, hAML lesions are always identified incidentally. Most hAMLs are solitary lesions, which could occur simultaneously to renal angiomyolipoma. About 80% of hAMLs could be found in tuberous sclerosis complex.

Imaging

Given their fat content, hAMLs usually show heterogenous and hyperechogenic on US [100]. Arterial blood flow signals with low RI can be detected. On CEUS, over 90% of hAMLs show heterogenous or homogenous hyperenhancement in the arterial phase; 2/3 of lesions show sustained hyperenhancement in the portal venous phase and late phase, while 1/3 show a wash-out [116] (fig 10).

Conclusion

Due to rarely conclusive diagnosis, overlap of imaging features, and malignant potential, the diagnosis of the majority of these lesions (hepatocellular adenoma, AML, PEComa, MCN-L) need biopsy and histochemical and molecular evaluation. In HCA the majority of subtypes at risk present with wash-out on CEUS. If the CEUS findings are consistent with CT/MRI findings biopsy may be skipped for some rare FLL (e.g., typical MCN-L with nodules iso- or hyperenhancing in the portal venous and late phase, hepatocellular adenoma <5 cm iso- or hyperenhancing in the portal venous and late phase), lipoma and bile duct hamartoma).

Conflict of interest: none. **Disclosures:** Some authors received speakers bureau and grants from Bracco and various ultrasound manufacturers.

References

1. Dietrich CF, Averkiou M, Nielsen MB, et al. How to perform Contrast-Enhanced Ultrasound (CEUS). Ultrasound Int Open 2018;4:E2-E15.
2. Claudon M, Dietrich CF, Choi BI, et al. Guidelines and good clinical practice recommendations for contrast enhanced ultrasound (CEUS) in the liver--update 2012: a WFUMB-EFSUMB initiative in cooperation with representatives of

AFSUMB, AIUM, ASUM, FLAUS and ICUS. Ultraschall Med 2013;34:11-29.
3. Claudon M, Dietrich CF, Choi BI, et al. Guidelines and good clinical practice recommendations for Contrast Enhanced Ultrasound (CEUS) in the liver - update 2012: A WFUMB-EFSUMB initiative in cooperation with representatives of AFSUMB, AIUM, ASUM, FLAUS and ICUS. Ultrasound Med Biol 2013;39:187-210.
4. Dietrich CF, Nolsoe CP, Barr RG, et al. Guidelines and Good Clinical Practice Recommendations for Contrast-Enhanced Ultrasound (CEUS) in the Liver-Update 2020 WFUMB in Cooperation with EFSUMB, AFSUMB, AIUM, and FLAUS. Ultrasound Med Biol 2020;46:2579-2604.
5. Dietrich CF, Nolsoe CP, Barr RG, et al. Guidelines and Good Clinical Practice Recommendations for Contrast Enhanced Ultrasound (CEUS) in the Liver - Update 2020 - WFUMB in Cooperation with EFSUMB, AFSUMB, AIUM, and FLAUS. Ultraschall Med 2020;41:562-585.
6. Moller K, Tscheu T, De Molo C, et al. Comments and illustrations of the WFUMB CEUS liver guidelines: rare congenital vascular pathology. Med Ultrason 2022;24:461-472.
7. Moller K, Braden B, Culver EL, et al. Secondary sclerosing cholangitis and IgG4-sclerosing cholangitis - A review of cholangiographic and ultrasound imaging. Endosc Ultrasound 2022, doi: 10.4103/EUS-D-22-00208.
8. Moller K, Safai Zadeh E, Gorg C, et al. Prevalence of benign focal liver lesions and non-hepatocellular carcinoma malignant lesions in liver cirrhosis. Z Gastroenterol 2022, doi: 10.1055/a-1890-5818.
9. Ignee A, Möller K, Thees-Laurenz R, et al. Comments and illustrations of the WFUMB CEUS liver guidelines: Rare focal liver lesions - infectious, bacterial. Med Ultrason 2023, doi: 10.11152/mu-4065.
10. Möller K, Stock B, Ignee A, et al. Comments and illustrations of the WFUMB CEUS liver guidelines. Rare focal liver lesion – non infectious, non-neoplastic. Med Ultrason. 2023, doi: 10.11152/mu-4192.
11. Zander T, Safai Zadeh E, Möller K, Goerg C, Correas JM, Chaubal N, et al. Comments and illustrations of the WFUMB CEUS liver guidelines: Infectious FLL parasitic and fungi. Med Ultrason. 2023, doi: 10.11152/mu-4091.
12. Moeller K, Safai Zadeh E, Goerg C, et al. Focal liver lesions other than hepatocellular carcinoma in cirrhosis: Diagnostic challenges. J Transl Int Med 2023;10:308-327.
13. Dong Y, Koch J, Alhyari A, et al. Ultrasound Elastography for Characterization of Focal Liver Lesions. Z Gastroenterol 2023;61:399-410.
14. Alhyari A, Gorg C, Alakhras R, Dietrich CF, Trenker C, Safai Zadeh E. HCC or Something Else? Frequency of Various Benign and Malignant Etiologies in Cirrhotic Patients with Newly Detected Focal Liver Lesions in Relation to Different Clinical and Sonographic Parameters. Diagnostics (Basel) 2022;12:2079.
15. Dong Y, Qiu Y, Zhang Q, et al. Preliminary Clinical Experience with Shear Wave Dispersion Imaging for Liver Viscosity in Preoperative Diagnosis of Focal Liver Lesions. Z Gastroenterol 2020;58:847-854.
16. Dong Y, Wang WP, Mao F, et al. Imaging Features of Fibrolamellar Hepatocellular Carcinoma with Contrast-Enhanced Ultrasound. Ultraschall Med 2020;42:306-313.
17. Safai Zadeh E, Baumgarten MA, Dietrich CF, et al. Frequency of synchronous malignant liver lesions initially detected by ultrasound in patients with newly diagnosed underlying non-hematologic malignant disease: a retrospective study in 434 patients. Z Gastroenterol 2022;60:586-592.
18. Chaubal N, Thomsen T, Kabaalioglu A, Srivastava D, Rosch SS, Dietrich CF. Ultrasound and contrast-enhanced ultrasound (CEUS) in infective liver lesions. Z Gastroenterol 2021;59:1309-1321.
19. Dong Y, Wang WP, Ignee A, et al. The Diagnostic Value of Doppler Resistive Index in the differential diagnosis of focal liver lesions. J Ultrason 2023, doi: 10.15557/JoU.2023.0010
20. Trenker C, Gorg C, Dong Y, et al. Portal venous gas detection in different clinical situations. Med Ultrason. 2023, doi: 10.11152/mu-4010.
21. Ignee A, Piscaglia F, Ott M, Salvatore V, Dietrich CF. A benign tumour of the liver mimicking malignant liver disease--cholangiocellular adenoma. Scand J Gastroenterol. 2009;44:633-636.
22. Gronlykke L, Tarp B, Dutoit SH, Wilkens R. Peliosis hepatis: a complicating finding in a case of biliary colic. BMJ Case Rep 2013;2013:bcr2013200539.
23. Loizides A, Glodny B, Zoller H, et al. Contrast enhanced ultrasound of a rare case of Peliosis hepatis. Med Ultrason 2017;19:114-116.
24. Dong Y, Wang WP, Lim A, et al. Ultrasound findings in peliosis hepatis. Ultrasonography 2021;40:546-554.
25. Dong Y, Wang WP, Mao F, et al. Contrast enhanced ultrasound features of hepatic cystadenoma and hepatic cystadenocarcinoma. Scand J Gastroenterol 2017;52:365-372.
26. Klinger C, Stuckmann G, Dietrich CF, et al. Contrast-enhanced imaging in hepatic epithelioid hemangioendothelioma: retrospective study of 10 patients. Z Gastroenterol 2019;57:753-766.
27. Dong Y, Wang WP, Cantisani V, et al. Contrast-enhanced ultrasound of histologically proven hepatic epithelioid hemangioendothelioma. World J Gastroenterol 2016;22:4741-4749.
28. Dong Y, Wang WP, Lee WJ, et al. Hepatocellular carcinoma in the non-cirrhotic liver. Clin Hemorheol Microcirc 2022;80:423-436.
29. Dong Y, Wang WP, Lee WJ, et al. Contrast-Enhanced Ultrasound Features of Histopathologically Proven Hepatocellular Carcinoma in the Non-cirrhotic Liver: A Multicenter Study. Ultrasound Med Biol 2022;48:1797-1805.
30. Moller K, Safai Zadeh E, Gorg C, et al. Focal Liver Lesions other than Hepatocellular Carcinoma in Cirrhosis: Diagnostic Challenges. J Transl Int Med 2022;10:308-327.
31. Fu T, Ding H, Xu C, Zhu Y, Xue L, Lin F. Imaging findings of fibrolamellar hepatocellular carcinomas on ultrasonogra-

phy: A comparison with conventional hepatocellular carcinomas. Clin Hemorheol Microcirc 2021;77:49-60.
32. Dong Y, Teufel A, Wang WP, Dietrich CF. Current Opinion about Hepatocellular Carcinoma <10 mm. Digestion 2021;102:335-341.
33. Dong Y, Teufel A, Trojan J, Berzigotti A, Cui XW, Dietrich CF. Contrast enhanced ultrasound in mixed hepatocellular cholangiocarcinoma: Case series and review of the literature. Dig Liver Dis 2018;50:401-407.
34. Faust D, Fellbaum C, Zeuzem S, Dietrich CF. Nodular regenerative hyperplasia of the liver: a rare differential diagnosis of cholestasis with response to ursodeoxycholic acid. Z Gastroenterol 2003;41:255-258.
35. Trojan J, Hammerstingl R, Engels K, Schneider AR, Zeuzem S, Dietrich CF. Contrast-enhanced ultrasound in the diagnosis of malignant mesenchymal liver tumors. J Clin Ultrasound. 2010;38:227-231.
36. Schuessler G, Fellbaum C, Fauth F, et al. [The infammatory pseudotumour -- an unusual liver tumour]. Ultraschall Med 2006;27:273-279.
37. Tana C, Schiavone C, Ticinesi A, et al. Ultrasound imaging of abdominal sarcoidosis: State of the art. World J Clin Cases 2019;7:809-818.
38. Tana C, Silingardi M, Dietrich CF. New trends in ultrasound of hepatosplenic sarcoidosis. Z Gastroenterol 2015;53:283-284.
39. Hirche TO, Hirche H, Cui XW, Wagner TO, Dietrich CF. Ultrasound evaluation of mediastinal lymphadenopathy in patients with sarcoidosis. Med Ultrason 2014;16:194-200.
40. Tana C, Dietrich CF, Schiavone C. Hepatosplenic sarcoidosis: contrast-enhanced ultrasound findings and implications for clinical practice. Biomed Res Int 2014;2014:926203.
41. Dong Y, Jurgensen C, Puri R, et al. Ultrasound imaging features of isolated pancreatic tuberculosis. Endosc Ultrasound 2018;7:119-127.
42. Barreiros AP, Braden B, Schieferstein-Knauer C, Ignee A, Dietrich CF. Characteristics of intestinal tuberculosis in ultrasonographic techniques. Scand J Gastroenterol 2008;43:1224-1231.
43. Dietrich CF, Douira-Khomsi W, Gharbi H, et al. Cystic echinococcosis, review and illustration of non-hepatic manifestations. Med Ultrason 2020;22:319-324.
44. Dietrich CF, Douira-Khomsi W, Gharbi H, et al. Cystic and alveolar echinococcosis of the hepatobiliary tract - the role of new imaging techniques for improved diagnosis. Med Ultrason 2020;22:75-84.
45. Brunetti E, Tamarozzi F, Macpherson C, et al. Ultrasound and Cystic Echinococcosis. Ultrasound Int Open 2018;4:E70-E8.
46. Dietrich CF, Mueller G, Beyer-Enke S. Cysts in the cyst pattern. Z Gastroenterol 2009;47:1203-1207.
47. Richter J, Botelho MC, Holtfreter MC, et al. Ultrasound assessment of schistosomiasis. Z Gastroenterol 2016;54:653-660.
48. Richter J, Azoulay D, Dong Y, et al. Ultrasonography of gallbladder abnormalities due to schistosomiasis. Parasitol Res 2016;115:2917-2924.
49. Dong Y, Mao F, Cao J, et al. Differential diagnosis of gallbladder ascariasis debris: the added value of contrast enhanced ultrasound with high frequency transducer. Med Ultrason 2018;20:413-419.
50. Dietrich CF, Sharma M, Chaubal N, et al. Ascariasis imaging: pictorial essay. Z Gastroenterol 2017;55:479-489.
51. Dietrich CF, Kabaalioglu A, Brunetti E, Richter J. Fasciolosis. Z Gastroenterol 2015;53:285-290.
52. Dietrich CF, Atkinson NSS, Lee WJ, et al. Never seen before? Opisthorchiasis and Clonorchiasis. Z Gastroenterol 2018;56:1513-1520.
53. Dietrich CF, Cretu C, Dong Y. Imaging of toxocariasis. Adv Parasitol. 2020;109:165-187.
54. Braden B, Helm B, Fabian T, Dietrich CF. [Bacillary angiomatosis of the liver, a suspected ultrasound diagnosis?]. Z Gastroenterol 2000;38:785-789.
55. Barreiros AP, Otto G, Ignee A, Galle P, Dietrich CF. Sonographic signs of amyloidosis. Z Gastroenterol 2009;47:731-739.
56. Chiorean L, Cui XW, Tannapfel A, et al. Benign liver tumors in pediatric patients - Review with emphasis on imaging features. World J Gastroenterol 2015;21:8541-8561.
57. Schreiber-Dietrich DG, Leuschner I, Tannapfel A, et al. [Primary liver tumours in childhood]. Z Gastroenterol 2015;53:1267-1275.
58. Nault JC, Paradis V, Cherqui D, Vilgrain V, Zucman-Rossi J. Molecular classification of hepatocellular adenoma in clinical practice. J Hepatol. 2017;67:1074-1083.
59. Nault JC, Couchy G, Balabaud C, et al. Molecular Classification of Hepatocellular Adenoma Associates With Risk Factors, Bleeding, and Malignant Transformation. Gastroenterology 2017;152:880-894.e6.
60. Grazioli L, Ambrosini R, Frittoli B, Grazioli M, Morone M. Primary benign liver lesions. Eur J Radiol 2017;95:378-398.
61. Farges O, Ferreira N, Dokmak S, Belghiti J, Bedossa P, Paradis V. Changing trends in malignant transformation of hepatocellular adenoma. Gut 2011;60:85-89.
62. Nault JC, Galle PR, Marquardt JU. The role of molecular enrichment on future therapies in hepatocellular carcinoma. J Hepatol 2018;69:237-247.
63. Nagtegaal ID, Odze RD, Klimstra D, et al. The 2019 WHO classification of tumours of the digestive system. Histopathology 2020;76:182-188.
64. Chen K, Dong Y, Zhang W, et al. Analysis of contrast-enhanced ultrasound features of hepatocellular adenoma according to different pathological molecular classifications. Clin Hemorheol Microcir 2020;76:391-403.
65. Dhingra S, Fiel MI. Update on the new classification of hepatic adenomas: clinical, molecular, and pathologic characteristics. Arch Pathol Lab Med 2014;138:1090-1097.
66. Bioulac-Sage P, Sempoux C, Balabaud C. Hepatocellular adenoma: Classification, variants and clinical relevance. Semin Diagn Pathol 2017;34:112-125.
67. Rebouissou S, Amessou M, Couchy G, et al. Frequent in-frame somatic deletions activate gp130 in inflammatory hepatocellular tumours. Nature 2009;457:200-204.

68. Rebouissou S, Imbeaud S, Balabaud C, et al. HNF1alpha inactivation promotes lipogenesis in human hepatocellular adenoma independently of SREBP-1 and carbohydrate-response element-binding protein (ChREBP) activation. J Biol Chem 2007;282:14437-1446.
69. Rebouissou S, Franconi A, Calderaro J, et al. Genotype-phenotype correlation of CTNNB1 mutations reveals different ss-catenin activity associated with liver tumor progression. Hepatology 2016;64:2047-2061.
70. Garcovich M, Faccia M, Meloni F, et al. Contrast-enhanced ultrasound patterns of hepatocellular adenoma: an Italian multicenter experience. J Ultrasound 2019;22:157-165.
71. Kim TK, Jang HJ, Burns PN, Murphy-Lavallee J, Wilson SR. Focal nodular hyperplasia and hepatic adenoma: differentiation with low-mechanical-index contrast-enhanced sonography. AJR Am J Roentgenol 2008;190:58-66.
72. Wang W, Liu JY, Yang Z, et al. Hepatocellular adenoma: comparison between real-time contrast-enhanced ultrasound and dynamic computed tomography. Springerplus 2016;5:951.
73. Laumonier H, Cailliez H, Balabaud C, et al. Role of contrast-enhanced sonography in differentiation of subtypes of hepatocellular adenoma: correlation with MRI findings. AJR Am J Roentgenol 2012;199:341-348.
74. Dietrich CF, Schuessler G, Trojan J, Fellbaum C, Ignee A. Differentiation of focal nodular hyperplasia and hepatocellular adenoma by contrast-enhanced ultrasound. Br J Radiol 2005;78:704-707.
75. Kong WT, Wang WP, Huang BJ, Ding H, Mao F, Si Q. Contrast-enhanced ultrasound in combination with color Doppler ultrasound can improve the diagnostic performance of focal nodular hyperplasia and hepatocellular adenoma. Ultrasound Med Biol 2015;41:944-951.
76. Zarzour JG, Porter KK, Tchelepi H, Robbin ML. Contrast-enhanced ultrasound of benign liver lesions. Abdom Radiol (NY) 2018;43:848-860.
77. Manichon AF, Bancel B, Durieux-Millon M, et al. Hepatocellular adenoma: evaluation with contrast-enhanced ultrasound and MRI and correlation with pathologic and phenotypic classification in 26 lesions. HPB Surg 2012;2012:418745.
78. European Association for the Study of the L. EASL Clinical Practice Guidelines on the management of benign liver tumours. J Hepatol 2016;65:386-398.
79. Kim TH, Woo S, Ebrahimzadeh S, McLnnes MDF, Gerst SR, Do RK. Hepatic Adenoma Subtypes on Hepatobiliary Phase of Gadoxetic Acid-Enhanced MRI: Systematic Review and Meta-Analysis. AJR Am J Roentgenol. 2023;220:456-457.
80. Reizine E, Ronot M, Pigneur F, et al. Iso- or hyperintensity of hepatocellular adenomas on hepatobiliary phase does not always correspond to hepatospecific contrast-agent uptake: importance for tumor subtyping. Eur Radiol 2019;29:3791-3801.
81. Moschcowitz E. Non-parasitic cyst (congenital) of the liver with a study of aberrant bile ducts. American Journal of the Medical Sciences 1906;131:674–699.
82. Meyenburg HV. Uber die Cystenleber. Beitr Pathol Anat 1918;64:477–532.
83. Redston MS, Wanless IR. The hepatic von Meyenburg complex: prevalence and association with hepatic and renal cysts among 2843 autopsies [corrected]. Mod Pathol 1996;9:233-237.
84. Guo Y, Jain D, Weinreb J. Von Meyenburg Complex: Current Concepts and Imaging Misconceptions. J Comput Assist Tomogr 2019;43:846-851.
85. Watanabe M, Shiozawa K, Ikehara T, et al. A case of solitary bile duct hamartoma with advanced gastric carcinoma: findings in contrast-enhanced ultrasonography. J Med Ultrason (2001) 2014;41:203-207.
86. Sasaki M, Sato Y, Nakanuma Y. Cholangiolocellular Carcinoma With "Ductal Plate Malformation" Pattern May Be Characterized by ARID1A Genetic Alterations. Am J Surg Pathol 2019;43:352-360.
87. Sasaki M, Sato Y, Nakanuma Y. Bile duct adenoma may be a precursor lesion of small duct type intrahepatic cholangiocarcinoma. Histopathology 2021;78:310-320.
88. Bhalla A, Mann SA, Chen S, Cummings OW, Lin J. Histopathological evidence of neoplastic progression of von Meyenburg complex to intrahepatic cholangiocarcinoma. Hum Pathol 2017;67:217-224.
89. Xu AM, Xian ZH, Zhang SH, Chen XF. Intrahepatic cholangiocarcinoma arising in multiple bile duct hamartomas: report of two cases and review of the literature. Eur J Gastroenterol Hepatol 2009;21:580-584.
90. Zheng RQ, Kudo M, Onda H, et al. Imaging findings of biliary hamartomas (von Meyenburg complexes). J Med Ultrason (2001). 2005;32:205.
91. Hohmann J, Loddenkemper C, Albrecht T. Assessment of a biliary hamartoma with contrast-enhanced sonography using two different contrast agents. Ultraschall Med 2009;30:18518-8.
92. Pech L, Favelier S, Falcoz MT, Loffroy R, Krause D, Cercueil JP. Imaging of Von Meyenburg complexes. Diagn Interv Imaging 2016;97:401-409.
93. Jaquez-Quintana JO, Reyes-Cabello EA, Bosques-Padilla FJ. Multiple Biliary Hamartomas, The ''Von Meyenburg Complexes''. Ann Hepatol 2017;16:812-813.
94. Monteiro de Barros J, Stell D, Bracey TS, Mavroeidis VK. Diffuse liver hamartomatosis (diffuse von Meyenburg complexes) mimicking hepatic metastases on a background of previous cancer. Ann R Coll Surg Engl 2020;102:e1-e4.
95. Lung PF, Jaffer OS, Akbar N, Sidhu PS, Ryan SM. Appearances of von Meyenburg complex on cross sectional imaging. J Clin Imaging Sci 2013;3:22.
96. Armutlu A, Quigley B, Choi H, et al. Hepatic Cysts: Reappraisal of the Classification, Terminology, Differential Diagnosis, and Clinicopathologic Characteristics in 258 Cases. Am J Surg Pathol 2022;46:1219-1233.
97. Ahmad Z, Uddin N, Memon W, Abdul-Ghafar J, Ahmed A. Intrahepatic biliary cystadenoma mimicking hydatid cyst of liver: a clinicopathologic study of six cases. J Med Case Rep 2017;11:317.

98. Jwa EK, Hwang S. Clinicopathological features and post-resection outcomes of biliary cystadenoma and cystadenocarcinoma of the liver. Ann Hepatobiliary Pancreat Surg 2017;21:107-113.
99. Valdivielso Cortazar E, Gonzalez Penas L, Alonso Aguirre P. Dilation of the biliary tract secondary to intrahepathic biliary mucinous cystadenoma with ovarian stroma. Rev Esp Enferm Dig 2021;113:470.
100. Nonomura A, Mizukami Y, Kadoya M. Angiomyolipoma of the liver: a collective review. J Gastroenterol 1994;29:95-105.
101. Soares KC, Arnaoutakis DJ, Kamel I, et al. Cystic neoplasms of the liver: biliary cystadenoma and cystadenocarcinoma. J Am Coll Surg 2014;218:119-128.
102. Xu HX, Lu MD, Liu LN, et al. Imaging features of intrahepatic biliary cystadenoma and cystadenocarcinoma on B-mode and contrast-enhanced ultrasound. Ultraschall Med 2012;33:E241-E9.
103. Williamson JM, Rees JR, Pope I, Strickland A. Hepatobiliary cystadenomas. Ann R Coll Surg Engl 2013;95:507-510.
104. Zhang FB, Zhang AM, Zhang ZB, et al. Preoperative differential diagnosis between intrahepatic biliary cystadenoma and cystadenocarcinoma: a single-center experience. World J Gastroenterol 2014;20:12595-601.
105. Lee CW, Tsai HI, Lin YS, Wu TH, Yu MC, Chen MF. Intrahepatic biliary mucinous cystic neoplasms: clinicoradiological characteristics and surgical results. BMC Gastroenterol 2015;15:67.
106. Thomas KT, Welch D, Trueblood A, et al. Effective treatment of biliary cystadenoma. Ann Surg 2005;241:769-773.
107. Emre A, Serin KR, Ozden I, et al. Intrahepatic biliary cystic neoplasms: Surgical results of 9 patients and literature review. World J Gastroenterol 2011;17:361-365.
108. Araujo RL, Cesconetto D, Jeismann VB, et al. Central Hepatectomy for Biliary Cystadenoma: Parenchyma-Sparing Approach for Benign Lesions. Arq Bras Cir Dig 2016;29:295-296.
109. Koffron A, Rao S, Ferrario M, Abecassis M. Intrahepatic biliary cystadenoma: role of cyst fluid analysis and surgical management in the laparoscopic era. Surgery 2004;136:926-936.
110. Pezzilli R, Buscarini E, Pollini T, et al. Epidemiology, clinical features and diagnostic work-up of cystic neoplasms of the pancreas: Interim analysis of the prospective PANCY survey. Dig Liver Dis 2020;52:547-554.
111. Brittingham C, Tuma F. Hepatic Cystadenoma. StatPearls. Treasure Island (FL) 2021.
112. Sato M, Watanabe Y, Tokui K, et al. Hepatobiliary cystadenocarcinoma connected to the hepatic duct: a case report and review of the literature. Hepatogastroenterology 2003;50:1621-1624.
113. Yang Y, Mai W, Chen W, Yang C, Li M, Liu L. Case Report: Low-Dose Apatinib in the Treatment of Intrahepatic Biliary Cystadenoma With Recurrence and Malignant Transformation. Front Oncol 2021;11:676092.
114. Karhunen PJ. Hepatic pseudolipoma. J Clin Pathol 1985;38:877-879.
115. Sachal M, Sohail AH, Khan MS, Memon W. Paracaval pseudolipoma mimicking intracaval mass lesion and thrombus. BMJ Case Rep 2018;2018:bcr2018225401.
116. Wang Z, Xu HX, Xie XY, et al. Imaging features of hepatic angiomyolipomas on real-time contrast-enhanced ultrasound. Br J Radiol 2010;83:411-418.